Proc. Natl. Acad. Sci. USA
Vol. 77, No. 6, pp. 3736–3740, June 1980
Neurobiology

Acetylcholine receptor site density affects the rising phase of miniature endplate currents

(α-bungarotoxin/voltage clamp/acetylcholine diffusion/neuromuscular junction/binding kinetics)

BRUCE R. LAND*, EDWIN E. SALPETER†, AND MIRIAM MARK SALPETER*‡

*Section of Neurobiology and Behavior, Division of Biological Science, and †Department of Physics, Cornell University, Ithaca, New York 14853

Contributed by Edwin E. Salpeter, March 24, 1980

ABSTRACT **The relationship between acetylcholine receptor (AcChoR) site density (σ) and the rising phase of the miniature endplate current was determined in esterase-inactivated lizard intercostal neuromuscular junctions. The currents were recorded by using a voltage clamp. The receptor site density was determined by electron microscope autoradiography after labeling with ^{125}I-labeled α-bungarotoxin in normal endplates and in those partially inactivated with nonradioactive α-bungarotoxin. We found that as σ is decreased the rise time is increased and the amplitude is decreased. These results are compatible with a previously stated "saturating disk" model, which suggests that a quantum of acetylcholine (AcCho) acts on a small postsynaptic area at saturating concentration. We conclude that in the normal neuromuscular junction the most likely number of AcCho molecules needed to open an ion channel is 2, and that the 20–80% rise time of <100 μsec is influenced both by the σ-dependent factors such as diffusion and binding of AcCho to AcChoR and by the σ-independent time delays such as the conformation change time to open the ion channels. From our data we calculate the lower limits to the forward rate constant of AcCho binding to AcChoR $\geq 3 \times 10^7$ M^{-1} sec^{-1}, and the diffusion constant for AcCho in the cleft $\geq 4 \times 10^{-6}$ cm^2 sec^{-1}.**

A unique molecular organization of acetylcholine receptors (AcChoRs) and acetylcholinesterase has been found in all neuromuscular junctions (nmjs) of vertebrate twitch muscles examined. This organization consists of a high and stable AcChoR site density σ of ≈20,000 sites/μm^2 of surface area at the top of the postjunctional membrane (1–4) and a uniform distribution of acetylcholinesterase of ≈2500 sites per μm^2 of surface area along the entire postjunctional folded membrane (5–8). In the present paper we attempt to determine some physiological consequences of this organization by studying the effect of decreasing σ on the rise time and amplitude of miniature endplate currents (mepcs) in esterase-inactivated nmjs. We found that, as σ is decreased, the rise time increases and the amplitude decreases. From these data we suggest some physiological parameters which control the action of acetylcholine (AcCho) in the cleft.

METHODS

Muscle Preparation. We used lizard (*Anolis carolinensis*) intercostal muscle. This muscle has compact endplates that are much smaller than the electrical length constant, and thus may be uniformly clamped. The muscle is thin (one to two fiber layers thick), allowing easy visualization of the endplates with Hoffman modulation optics. The physiological studies were performed on endplates pretreated with diisopropylfluorophosphate (iPr_2P-F) (1 mM for 20 min), which effectively inactivates esterases. The AcChoRs were either left intact or were partially inactivated with α-bungarotoxin (BTX) (9) (40 nM) for 20 or 40 min. The muscle was thoroughly washed (30 min) to remove excess iPr_2P-F and BTX. The mepcs were measured in fibers that had been voltage clamped at −100 mV (23°C), using 3–6 MΩ electrodes. The clamp output was passed through a two-pole Butterworth lowpass filter with 4-kHz cut-off to remove high-frequency noise. Approximately two hundred mepcs were obtained from each fiber. After the physiological recordings, the muscles were incubated in ^{125}I-labeled BTX (^{125}I-BTX) (500 nM) for 2 hr, as described for the frog (4), and prepared for electron microscope autoradiography by the flat substrate procedure of Salpeter and Bachmann (10, 11), using Ilford L4 emulsion and D-19 development (2 min at 20°C). In order to determine that there was no loss of BTX during the 6 hr before fixation while the physiological studies were performed, control preparations were labeled with ^{125}I-BTX (500 nM) immediately after the incubation with the nonradioactive BTX.

Improving Resolution of mepc Rise Time Data. For these studies we needed an undistorted record of the average mepc rise time. To obtain this, several procedures were followed: (*i*) We drained the dish during recording in order to lower electrode capacitance to ground (100–200 μm of liquid was left over the cells); we calculate that the small fluid layer increased the total resistance by less than 10%. (*ii*) We penetrated the cell within one fiber diameter of the nmj. (*iii*) We used a 4-kHz filter and digitized the current waveform at 40,000 samples per sec. (*iv*) We injected a 1-mV command voltage to the clamp and measured the actual voltage rise time prior to recording the mepcs. (*v*) Cells were used only if the clamped voltage change was less than 5% of the unclamped miniature endplate potential amplitude. These procedures allowed us to obtain a fast (20 μsec) clamp rise time (20–80%) and to minimize distortion of the mepc waveform but left us with a noisy signal. We therefore used averaging of the traces to resolve the signal. Because mepcs are spontaneous random events, the individual traces were aligned before averaging, using a two-step procedure. First each raw trace was smoothed by using a 16-point running average, which lengthens the rise time artifactually but leaves the amplitude and "half-time point" (the time when half of the peak

The publication costs of this article were defrayed in part by page charge payment. This article must therefore be hereby marked "*advertisement*" in accordance with 18 U. S. C. §1734 solely to indicate this fact.

Abbreviations: mepc, miniature endplate current; A, mepc amplitude; t_r, 20–80% rise time of a mepc; AcCho, acetylcholine; AcChoR, acetylcholine receptor; σ, AcChoR binding sites per μm^2; BTX, α-bungarotoxin; nmj, neuromuscular junction; iPr_2P-F, diisopropylfluorophosphate.

‡ To whom reprint requests should be addressed.

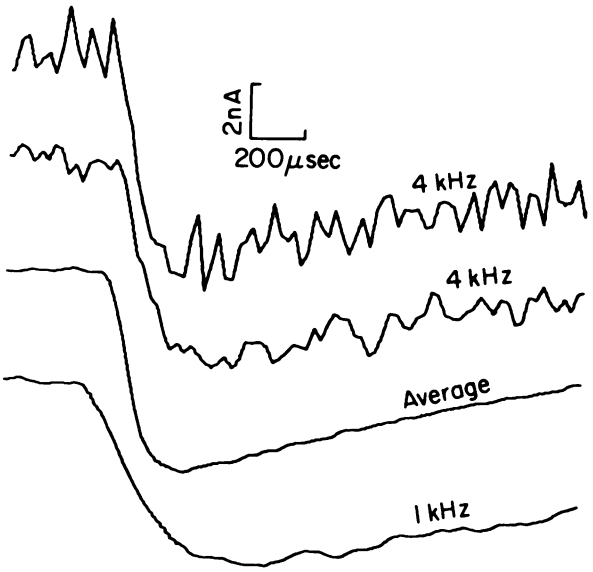

FIG. 1. Effects of averaging and filtering on mepc shape. The two top traces are randomly chosen raw mepc waveforms (of approximately the same amplitude as that of the average) to illustrate the recording noise at 4-kHz bandwidth. The third trace consists of ≈500 mepcs recorded at 4-kHz bandwidth and averaged as described in the text. Note that the alignment of traces was good enough so that the fast rising phase was not "smeared." The fourth trace is a single mepc waveform after heavier filtering (1-kHz bandwidth), which also suppresses noise but lengthens the rising time significantly.

amplitude is reached) relatively unaltered. The smoothed traces were used only to provide the "half-time point" onto which the original unsmoothed mepcs were then aligned and computer averaged. We thus obtained an improved signal-to-noise ratio without major distortion of the rising phase of the mepc (top three traces, Fig. 1). By contrast, a single mepc after 1-kHz filtering also has low noise but is broadened appreciably (bottom trace, Fig. 1).

RESULTS

Fig. 2 shows an autoradiogram of a lizard intercostal nmj treated with ^{125}I-BTX. Electron microscope autoradiographic

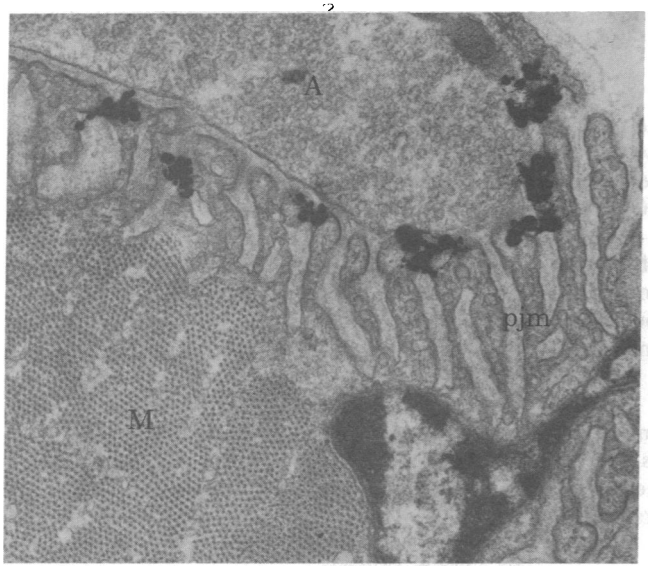

FIG. 2. Electron microscope autoradiogram of lizard endplate labeled with ^{125}I-BTX. A, axon; M, muscle; pjm, postjunctional fold. (Ilford L4 emulsion; D-19 development; ×24,000.)

Table 1. The mepc amplitude (A) and 20–80% rise time (t_r) for various AcChoR (BTX)-binding site densities (σ) in esterase-inactivated endplates

Condition	A, nA	t_r, μsec	σ, sites/μm^2
iPr_2P-F only	7.5 ± 1.3	91 ± 16	18,000 ± 4,000
iPr_2P-F + 20-min BTX	4.0 ± 0.7	160 ± 25	8,200 ± 1,900
iPr_2P-F + 40-min BTX	2.5 ± 0.5	196 ± 25	6,900 ± 2,000

Error limits as explained for Fig. 3. Where indicated, BTX (40 nM) was present for 20 or 40 min.

analysis indicated that the mean AcChoR site density is approximately 18,000 sites/μm^2 of specialized dense membrane at the top of the junctional folds and thus similar to values for mouse and frog.§ Furthermore, using previously described techniques (5–8), we have recently found that there are ≈3000 acetylcholinesterase sites per μm^2 of postjunctional membrane in the lizard nmj (unpublished). The molecular organization of the lizard intercostal nmj is thus essentially the same as that of the mouse and frog muscles studied to date.

Table 1 summarizes both the autoradiographic and physiological data. Note that the average t_r (defined as the 20–80% rise time) for normal nmjs (treated with iPr_2P-F only) is <100 μsec. This value is in line with that obtained by Gage and McBurney (13), and with the values used in mathematical modeling of the mepc (14). It is, however, considerably faster than the value often reported in the literature (15, 16), perhaps due to the procedures described above for obtaining a better time resolution. Table 1 also shows that the t_r increased when the muscle was incubated with BTX. [A similar observation was made by Katz and Miledi when using curare (17).]

Fig. 3 gives the relationship between t_r and σ for averaged values obtained from several muscles after three different inactivation conditions, and Fig. 4 gives the relationship between mepc amplitude (A) and σ. We see that t_r increases and A decreases as σ is decreased by BTX inactivation. The stated errors in Table 1 (and Figs. 3 and 4) are estimated standard errors, including formal statistical errors plus estimates for possible systematic errors.

DISCUSSION

"Saturating Disk" Model. We shall discuss the relationships between t_r, A, and σ in Figs. 3 and 4 in the framework of a model to be called the "saturating disk" model, which was proposed in earlier studies from this laboratory (3, 4). This model states that the high AcChoR binding site density allows a quantal packet of AcCho to be essentially fully bound within a small postsynaptic area and thus act at saturating concentration. [Adams (18) also favors such a model.] More specifically, let a_q be the postsynaptic area (to be called the minimum quantal area), which contains the number of AcChoR binding sites equal to the number, N, of AcCho molecules in a quantal packet (thus $a_q = N/\sigma$). Then, for the normal AcChoR site density, $\sigma \approx 20{,}000$ sites per μm^2, and a quantal packet of $N = 10^4$ AcCho molecules (e.g., see ref. 19), a_q is ≈0.5 μm^2. With a cleft thickness of 50 nm, a quantal packet of AcCho will act over a_q at an average concentration above 500 μM, which is indeed higher than the highest published values of the dissociation constant for binding of AcCho to AcChoR (20). Similar

§ Previous values for AcChoR density published from this laboratory (3, 4) were ≈30% too high due to a net effect of two systematic errors. The major one was our use of bovine serum albumin as the standard for the Lowry protein determination, which gives an overestimate of BTX protein concentration (unpublished data). In addition, we now make a slight correction for self-absorption of ^{125}I in 100-nm stained autoradiographic sections (12).

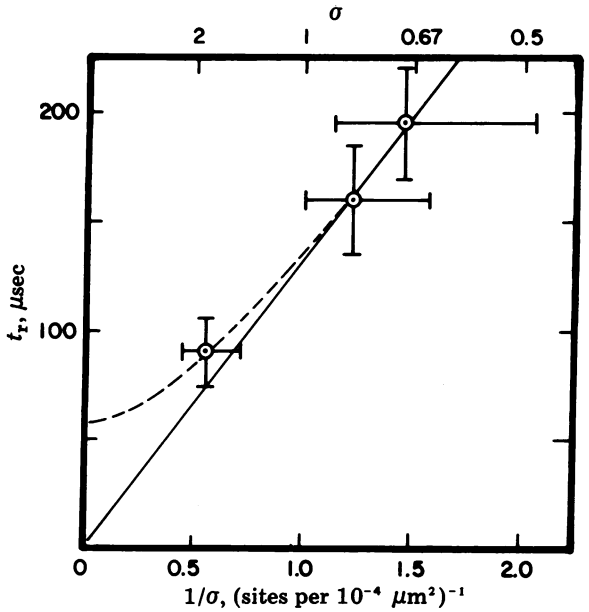

FIG. 3. t_r versus $1/\sigma$ in esterase-inactivated endplates. The mean values (± one standard error) are given for each of the three experimental conditions (0, 20, and 40 min in BTX). The solid curve is a straight line fit forced to pass through the origin; the broken curve is a fit, described in Eq. 2, that includes an exponential relaxation term for the opening of the receptor channel. The mean values include 7 preparations on which both physiological measurements and electron microscope and autoradiography were performed and 20 preparations on which only physiological measurements were performed.

high local AcCho concentrations per quantal packet were also suggested by Hartzell *et al.* (15) and by Lester *et al.* (21). As we discuss later, saturating AcCho concentration does not necessarily mean that all the AcChoR within area a_q are occupied. It does mean, however, that the forward rate of AcCho binding to AcChoR is much faster than the back reaction and that little AcCho will remain unbound in the cleft at the peak of the rising phase of a mepc.

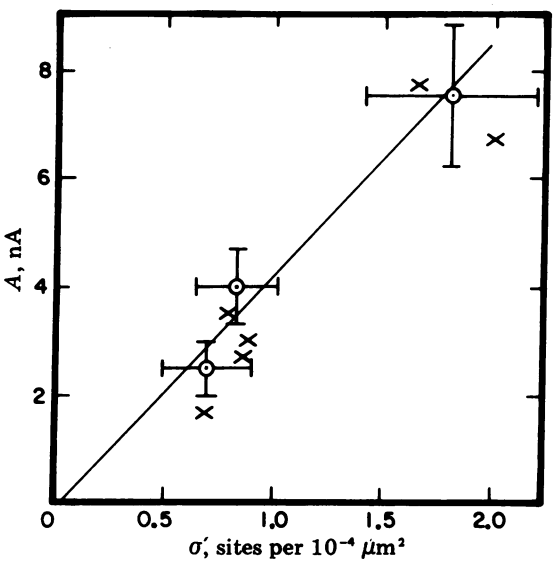

FIG. 4. A versus σ. The three points with error bars are the averaged preparations as in Fig. 3. The single points (×) represent the individual preparations from which both autoradiographic and mepc data were obtained. The line is the best fit forced to pass through the origin.

Rise Time–σ Correlation. We observed in Fig. 3 that t_r is almost proportional to $1/\sigma$. The saturating disk model predicts such a relationship under certain conditions. Consider that t_r can be controlled by the time (t_{b+d}) for a quantum of AcCho to diffuse to and bind to the postsynaptic AcChoRs, as well as by some time delay (t_c) contributed by various factors such as AcCho release but primarily by channel opening. Let t_d (to be defined more quantitatively in Eq. 5) be a characteristic time for AcCho to diffuse over the minimum area $a_q = N/\sigma$. Because diffusion time is proportional to area covered, t_d is proportional to $1/\sigma$. Let t_b (to be defined more quantitatively in Eq. 4) be a characteristic time for an AcCho molecule to bind to AcChoR in the absence of competition for binding sites. Because the forward binding rate is proportional to the rate constant (k_+) and to the concentration of the reactant AcChoR, the time t_b is also proportional to $1/\sigma$. The combined diffusion and binding component (t_{b+d}) of t_r is then also of the form

$$t_{b+d} = C/\sigma, \qquad [1]$$

in which C is a proportionality constant.

We have emphasized that the AcChoR sites within the minimum area a_q need not necessarily be fully bound. If binding is slower than diffusion ($t_b \gg t_d$), a steady state is not reached during the mepc rise time and the actual effective area (to be called a_e) over which the quantum is bound is larger than a_q. Eq. 1 will, however, still hold as long as the AcCho remains at saturating concentrations and is not lost from the cleft during t_r. The saturating disk model thus predicts that t_r will be proportional to $1/\sigma$ provided t_r is controlled by t_{b+d} and is not dominated by any σ-independent time delays. In Fig. 3 any effect of σ-independent time delays should be most noticeable at low values of $1/\sigma$ in the form of an upward deviation from linearity, giving a positive y intercept. Any effect of AcCho loss from the cleft or decreasing efficiency of binding due to decreased AcChoR concentration should be most noticeable at large values of $1/\sigma$ as a decreasing slope.

The solid straight line drawn in Fig. 3 is a best fit line, forced to go through the origin to accentuate any experimental deviation from proportionality. No deviation is apparent at large values of $1/\sigma$ (which is consistent with saturating AcCho concentration and no loss of AcCho). There is a small, upward deviation from proportionality at small values of $1/\sigma$, suggesting the presence of a positive t_c. If we assume that t_c reflects the conformational change in the ion channel, it can be modelled as an exponential relaxation, $\exp(-l_r t)$, in which l_r equals the relaxation rate constant.

In the limit when $1/\sigma \to 0$, the rising phase of a mepc would be controlled solely by this relaxation phenomenon. The t_r would then equal $t_c = 1.39/l_r$, in which 1.39 is ln(80/20), the conversion factor from the exponentiation time constant to the 20–80% rise time. With large values of $1/\sigma$ the rising phase of a mepc will reflect a time development due to the combined effect of t_c and t_{b+d}. With a simple analytic fit to the waveform of a mepc and an assumed exponential relaxation, computer calculations showed that t_r is given to a good approximation by the quadratic form:

$$t_r \approx [t_c^2 + (C/\sigma)^2]^{1/2}, \qquad [2]$$

in which C is defined in Eq. 1. (Note that the effect of t_c on t_r is small for large values of $1/\sigma$.) A maximum likelihood procedure, applied to the three points (plus error bars) in Fig. 3 gave the following fit to the two parameters:

$$t_c = (58 \pm 16)\mu\text{sec},$$
$$C = (1.24 \pm 0.25) \times 10^6 \mu\text{sec}/\mu\text{m}^2. \qquad [3]$$

For the normal nmj, Eq. 3 gives $C/\sigma \approx 68$ μsec. The "standard

errors" in Eq. 3 include the random errors obtained from the maximum likelihood procedure and the estimated systematic calibration errors. The broken curve in Fig. 3 shows the fit from Eqs. 2 and 3. If we assume that t_c is primarily due to the conformational change of the AcChoR–channel complex, then $t_c/1.39 = 1/l_r = 42 \pm 12$ μsec. If any other σ-dependent time delays contribute to t_c, then the 42 μsec is an upper limit to the relaxation time constant for the AcChoR gating. Although the relaxation rate l_r is the sum of the rates for gate opening (l_+) and closing (l_-), we shall demonstrate (in a later paper) that the high efficiency of an AcCho quantal response requires that l_- be small compared to l_+ and that the 42 μsec reflects primarily the gate opening time constant.

Limits to Kinetic Parameters in the Cleft. At present our data do not allow us to separate the influence on t_r of diffusion and binding. However, the value of C/σ (Eq. 1) can give an upper limit to both t_b and t_d, and hence we can derive the lower limits to the forward rate constants (k_+) for AcCho binding to AcChoR and the diffusion constant (D) for AcCho diffusion in the cleft.

The upper limit for t_b would be attained if diffusion were rapid relative to binding ($t_d \ll t_b$). In that case there would be little competition for AcChoR sites (AcCho would spread over an area $a_e \gg a_q$) and, in the limit of $t_b \gg t_d$, $t_b = t_{b+d} = C/\sigma$. But t_b is, by definition, proportional to $h/(\sigma k_+)$, in which h is the height of the cleft and σ/h is the effective concentration of AcChoR. Then, when binding is rate limiting, the 20–80% rise time is:

$$t_r = t_b = C/\sigma = 1.39h/\sigma k_+ \quad [4]$$

The 1.39 is the conversion factor from the exponential time constant for the decay of free AcCho to the 20–80% rise time.

From our measured value of C given in Eq. 3 (plus 2.5 times the standard deviation) we then get that $k_+ \geq 3 \times 10^7$ M^{-1} sec^{-1}. This inequality is altered only slightly if the number (n) of AcCho binding sites per AcChoR–channel complex is larger than 1. For instance, if $n = 2$ (with or without cooperativity in binding), the forward rate constant for the *first* binding satisfies $k_+ \geq (3/2) \times 10^7$ M^{-1} sec^{-1}. For comparison, Wathey *et al.* (14) use a rate constant of 3×10^8 M^{-1} sec^{-1} for the first of two binding steps, and Rosenberry (22) uses a forward rate constant of 2×10^7 M^{-1} sec^{-1}.

The value for t_d would reach its upper limit if binding were fast relative to diffusion: In the limit of $t_b \ll t_d$, $a_e = a_q$ and, from Eq. 1, $t_d = t_{d+b} = C/\sigma$. Diffusion time is proportional to area covered divided by the diffusion constant D. But, by definition, $a_q = N/\sigma$. Thus, in the limit of infinitely fast binding when diffusion rate is limiting, the 20–80% rise time is

$$t_r = t_d = C/\sigma = K(N/\sigma D), \quad [5]$$

in which K is a proportionality constant. We used a computer model (to be described in a later paper) to solve the diffusion equation extrapolated to rapid binding, and obtained a value for K of about 0.06. With $N = 10^4$ AcCho molecules in a quantal packet (19) and using the upper limit of C (Eq. 3), we calculated $D \geq 4 \times 10^{-6}$ cm^2 sec^{-1}. This lower limit to the diffusion constant is about half that given for free diffusion by Krnjevic and Mitchell (23) and is similar to the value quoted by Wathey *et al.* (14).

There is now general agreement (3, 4, 15, 18, 21) that a quantum of AcCho can act over a small postsynaptic area at high (saturating) concentrations, but, as we already stated, it does not necessarily follow that all the AcChoR within this area need actually be bound. If $t_d \ll t_b \approx t_{b+d}$, then a_e is larger than the minimum area a_q, by approximately t_b/t_d. The extent of AcChoR saturation is not known, but two indirect arguments on this point can be made: (*i*) Hartzell *et al.* (15) find that the postsynaptic response due to an iontophoretically applied AcCho pulse adds linearly to that of a quantum of AcCho without a significant increase in time to peak. This result is compatible with an unsaturated disk—i.e., $a_e \gg a_q$ (linear part of the dose–response curve) but does not require it. Because their iontophoretic AcCho covered a large area at low concentration, it would bind a small fraction of AcChoRs within any postsynaptic area. In order to produce its full response, and add linearly to the iontophoretic response, the quantum of AcCho needs only to spread over a disk area larger than its normal a_e by this small fraction. (*ii*) The fact that t_r does not deviate significantly from proportionality with $1/\sigma$ at the smallest values of σ used in our experiment means that AcCho remains saturating and that little AcCho is wasted by leakage from the cleft during t_r. The smallest values of σ in our BTX-inactivated nmjs gives an a_q with a radius of ≈0.7 μm. We estimate that this must be approaching the morphological dimensions of the cleft, and therefore that a_e cannot be much larger than a_q.

Amplitude–σ Correlation. We observed in Fig. 4 that the amplitude was roughly proportional to σ. This type of relationship is predicted from the saturating disk model, provided the number (n) of AcCho binding sites needed to open the ion channel is larger than 1 (and, for the simplest assumption that binding to one site does not affect binding to other sites, n is equal to 2). A conclusion that $n > 1$, and that most likely $n = 2$, is consistent with physiological (18, 20, 24), biochemical (25, 26), and morphological studies (27).

The justification for our conclusions from the amplitude–σ correlations is as follows: As σ is decreased, the AcCho packet has to spread further and takes longer to bind, but as long as the AcCho concentration remains high and AcCho is not yet lost from the cleft (which we have claimed above is the case in our experiments), the AcCho molecules will eventually be bound somewhere within the area a_e. If $n = 1$, then each AcCho molecule, once bound, would have an equal chance of opening a channel and A should not decrease with decreasing σ. If, however, $n > 1$, then any AcCho molecule that binds to an AcChoR–channel complex that already has BTX bound to one of its other binding sites cannot open a channel and is wasted. Therefore, when σ is decreased by BTX binding, A will also decrease. Because this is what we observe, most channel openings must go with $n > 1$. Our results are, however, not accurate enough to exclude a small probability of opening some AcChoR channels with only one AcCho bound to an AcChoR-channel complex (28).

More quantitatively, let σ_o = the original density of AcChoR binding sites and q = the fraction of sites available for AcCho binding after BTX. Then $q = \sigma/\sigma_o$, and (without cooperativity in binding) q^n = the fraction of AcChoR-channel complexes with all n sites available for binding. Because A (the number of open channels) $\propto (q^n a_e)$ and $a_e \propto 1/\sigma$, $\therefore A \propto q^n/\sigma$ or σ^{n-1}. Thus for $n = 1$, A should be independent of σ; for $n = 2$ (without cooperativity in binding) A should be proportional to σ, as we obtained in Fig. 4; and for $n > 2$, A should decrease faster than σ.

On the other hand, the saturating disk model makes a different prediction for the relationship between A and σ if σ is decreased due to the elimination or inactivation of entire AcChoR–channel complexes rather than due to the random elimination of individual AcChoR binding sites as it is by BTX. In that case, even if σ is decreased by a factor of 2 or 3, A (in the absence of acetylcholinesterase) would not decrease whatever the value for n, because none of the AcCho is wasted by binding

to partially inactivated AcChoR–channel complexes. This argument has to be modified if AcCho is lost during t_r by leakage from the cleft. Then a further decrease of AcChoR–channel complexes would result in a decrease in A and a loss in linearity between t_r and $1/\sigma$. Such seems to be the case in the numerical calculations of Wathey *et al.* (14), in which a small ($\approx$0.5 μm) cleft radius is assumed. However, a more general prediction that the time derivative dA/dt at early times is proportional to σ should hold in this case whether there is leakage from the cleft or not.

SUMMARY AND CONCLUSION

In summary, when AcChoR binding site density (σ) is decreased by BTX in esterase-inactivated lizard intercostal endplates, the mepcs rise times lengthen almost proportionately with $1/\sigma$. Such a relationship is predicted by the saturating disk model, which requires that a packet of AcCho act during t_r at a concentration well above its dissociation constant for binding AcChoR and be initially bound without a significant loss from the cleft. We conclude that at a normal nmj the σ-dependent factors (such as the time for AcCho to diffuse to or to bind to the AcChoR) and σ-independent time delays (such as the time to open the receptor-linked ion channel) both influence the rising phase. However, when σ is reduced by as little as a factor of 2 or 3, the σ-dependent factors dominate. Furthermore, the dependence of amplitude on σ, seen in Fig. 4, is predicted by our model provided the number of AcCho binding sites necessary to open the AcChoR linked ion channel is greater than 1, and is probably 2.

An AcChoR–channel complex with $n > 1$ would tend to suppress the endplate response to a low concentration AcCho leakage (29). However, for AcCho released in concentrated quantal packets, the molecular organization of high σ ensures that the AcCho can be bound over a small postsynaptic area at saturating concentration. Thus, the small postsynaptic area ensures fast time response and the saturating AcCho concentration ensures a high binding efficiency, which is particularly important with $n > 1$.

The saturating disk model, which was proposed on the basis of molecular anatomy (3, 4) appears to be compatible with our data. In the present study it has provided a basis for calculating approximate values for the conformational ion gate opening and lower limits to the forward binding rate constant and for the diffusion constant for AcCho in the cleft. We can now expect it to provide a guide for further experiments and for computer modeling, which should give actual values for the kinetic parameters operating in an intact nmj.

We thank Charles Stevens for giving us the voltage clamp design, Ralph Loring for preparing the BTX, Henry Lester for helpful discussions, and Maria Szabo, Mary Johnson, and Joyce Davis for technical assistance. This research was carried out during the tenure of a Postdoctoral Fellowship from the Muscular Dystrophy Association (to B.R.L.) and was supported in part by Grant NS 09315 from the National Institutes of Health. This work was presented in preliminary form at the Society for Neuroscience meeting, 1978.

1. Fertuck, H. C. & Salpeter, M. M. (1974) *Proc. Natl. Acad. Sci. USA* **71,** 1376–1378.
2. Porter, C. W. & Barnard, E. A. (1975) *J. Membr. Biol.* **14,** 383–401.
3. Fertuck, H. C. & Salpeter, M. M. (1976) *J. Cell Biol.* **69,** 144–158.
4. Mathews-Bellinger, J. & Salpeter, M. M. (1978) *J. Physiol.* **279,** 197–213.
5. Rogers, A. W., Darzynkiewicz, Z., Salpeter, M. M., Ostrowski, K., & Barnard, E. A. (1969) *J. Cell Biol.* **41,** 665–685.
6. Salpeter, M. M. (1969) *J. Cell Biol.* **42,** 122–134.
7. Salpeter, M. M., Plattner, H. & Rogers, A. J. (1972) *J. Histochem. Cytochem.* **12,** 1059–1068.
8. Salpeter, M. M., Rogers, A. W., Kasprzak, H. & McHenry, F. A. (1978) *J. Cell Biol.* **78,** 274–285.
9. Lee, C. Y., Chang, S. L., Kau, S. T. & Lau, S. H. (1972) *J. Chromatogr.* **72,** [illegible]82.
10. Salpeter, M. M. & Bachmann, L. J. (1964) *J. Cell Biol.* **22,** 469–476.
11. Salpeter, M. M. (1966) in *Methods in Cell Physiology,* ed. Prescott, D. (Academic, New York), Vol. 2, pp. 229–253.
12. Fertuck, H. C. & Salpeter, M. M. (1974) *J. Histochem. Cytochem.* **22,** 80–87.
13. Gage, P. W. & McBurney, R. N. (1975) *J. Physiol.* **244,** 385–407.
14. Wathey, J. C., Nass, M. M. & Lester, H. S. (1979) *Biophys. J.* **27,** 145–164.
15. Hartzell, H. C., Kuffler, S. W., & Yoshikami, D. J. (1975) *J. Physiol.* **251,** 427–463.
16. Cull-Candy, S. G., Miledi, R., & Trautmann, A. (1979) *J. Physiol.* **287,** 247–265.
17. Katz, B. & Miledi, R. J. (1973) *J. Physiol.* **231,** 549–574.
18. Adams, P. R. (1980) in *Information Processing in the Nervous System,* eds. Pinsker, H. M. & Willis, W. D., Jr. (Raven, New York), pp. 109–124.
19. Kuffler, S. W. & Yoshikami, D. J. (1975) *J. Physiol.* **251,** 465–482.
20. Colquhoun, D. (1979) in *The Receptors: A Comprehensive Treatise,* ed. O'Brien, R. D. (Plenum, New York), Vol. 1, pp. 93–142.
21. Lester, H. A., Koblin, D. D. & Sheridan, R. E. (1978) *Biophys. J.* **21,** 181–194.
22. Rosenberry, T. L. (1979) *Biophys. J.* **26,** 263–290.
23. Krnjevic, K. & Mitchell, J. F. (1960) *J. Physiol.* **153,** 562–572.
24. Adams, P. R. (1975) *Pflügers Arch.* **360,** 145–153.
25. Sobel, A., Weber, M. & Changeux, J.-P. (1977) *Eur. J. Biochem.* **80,** 215–224.
26. Neubig, R. R. & Cohen, J. B. (1979) *Biochemistry* **24,** 5465–5475.
27. Heuser, J. E. & Salpeter, S. R. (1979) *J. Cell Biol.* **82,** 150–173.
28. Dionne, V. E., Steinbach, J. H. & Stevens, C. F. (1978) *J. Physiol.* **281,** 421–444.
29. Katz, B. & Miledi, R. (1977) *Proc. R. Soc. London Ser. B* **196,** 59–72.